Bis(imido) W(VI) Complexes Chelated by N,N′-Disubstituted 1,8-Diamidonaphthalene: An Analysis of Bonding, Isocyanate Insertion, and Al-Me Transfer

Nathalie Lavoie, Tiow-Gan Ong,*,† Serge I. Gorelsky, Ilia Korobkov, Glenn P. A. Yap,‡ and Darrin S. Richeson*

Department of Chemistry and the Center for Catalysis Research and Innovation, University of Ottawa, Ottawa, Ontario, Canada K1N 6N5, Institute of Chemistry, Academia Sinica, Taipei, Taiwan 11529, and Department of Chemistry and Biochemistry, University of Delaware, Newark, Delaware 19716

Received July 27, 2007

Bis(imido)W(VI) complexes of dianionic N,N′-disubstituted 1,8-diamidonaphthalene (R_2DAN^{2-}) (R = ^{i}Pr, 3,5-$Me_2C_6H_3$) are reported, and an X-ray structure and computational analysis of W(=N^{t}Bu)$_2$[1,8-(^{i}PrN)$_2C_{10}H_6$] ***1*** revealed that the nonplanar coordination of the ^{i}Pr$_2$DAN^{2-} ligand to the W center is favored to allow for increased electron donation from the amido N centers to the W. Experimental studies revealed that the R_2DAN^{2-} amido linkage is the preferred reaction site with isocyanates to yield tridentate amido/*N*,*N*′-ureato ligands and that reactions with Al_2Me_6 lead to methylation of W and formation of heterobimetallic species via a μ^2-bridging interaction of the R_2DAN^{2-} ligand.

Introduction

A primary incentive for the design and development of new ligand arrays centers on attempts to manipulate the structure, stability, and reactivity of coordination compounds. The nature of the ligand functional groups and the ligand framework essentially define these characteristics. As an example, β-diketiminates have a documented role as supporting ligands due to their strong metal binding in combination with their adjustable steric demands and their diversity of bonding modes.[1] We are interested in designing and implementing a new family of dianionic ligands that are reminiscent of the β-diketiminate scaffold in geometry and frontier orbital topology. This led us to an array that is built on the N,N′-substituted 1,8-diamidonaphthalene framework (R_2DAN^{2-}), a rigid chelating ligand with delocalized π-electrons.[2,3] Among the significant differences between these two ligands are the dianionic charge and the naphthalene backbone of R_2DAN^{2-}. We anticipated that this first feature would allow the application of this ligand to metal complexes in their highest oxidation states and the second feature would lead to a more robust ligand relative to β-diketiminate.[4]

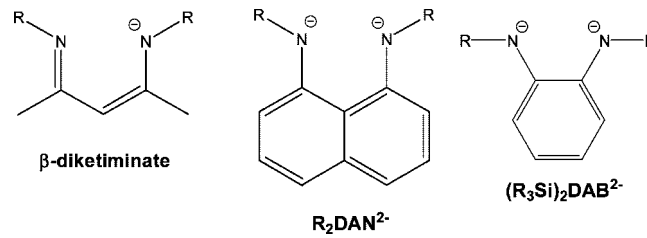

Additional inspiration for our investigations with R_2DAN^{2-} comes from the application of related chelating aromatic diamido ligands *N*,*N*′-bis(trialkylsilyl)-*o*-diamidobenzene ($(R_3Si)_2DAB^{2-}$) for the preparation of high-valent group 4,[5] Ta,[6] Mo, and W(VII) species. While having the same ligand charge, the diamidobenzene and diamidonaphthalene species exhibit substantially different topologies which should markedly influence the reactivity of their respective metal complexes.

This report extends our continuing examination of R_2DAN^{2-} ligands to their application with imido tungsten(VI) complexes.

* To whom correspondence should be addressed. E-mail: darrin@uottawa.ca.
† Academia Sinica.
‡ University of Delaware.

(1) (a) For recent reviews of β-diketiminates and their metal complexes, see: Bourget-Merle, L.; Lappert, M. F.; Severn, J. R. *Chem. Rev.* **2002**, *102*, 3031. (b) Gibson, V. C.; Spitzmesser, S. K. *Chem. Rev.* **2003**, *103*, 283. (c) Dechy-Cabaret, O.; Martin-Vaca, B.; Bourissou, D. *Chem. Rev.* **2004**, *104*, 6147.

(2) (a) Bazinet, P.; Yap, G. P. A.; DiLabio, G. A.; Richeson, D. S. *Inorg. Chem.* **2005**, *44*, 4616. (b) Bazinet, P.; Yap, G. P. A.; Richeson, D. S. *J. Am. Chem. Soc.* **2003**, *125*, 13314. (c) Bazinet, P.; Yap, G. P. A.; Richeson, D. S. *Organometallics* **2001**, *20*, 4129. (d) Bazinet, P.; Yap, G. P. A.; Richeson, D. S. *J. Am. Chem. Soc.* **2001**, *123*, 11162.

(3) For selected applications of R_2DAN^{2-}, see: (a) Danièle, S.; Drost, C.; Gehrhus, B.; Hawkins, S. M.; Hitchcock, P. B.; Lappert, M. F.; Merle, P. G.; Bott, S. G. *J. Chem. Soc., Dalton Trans.* **2001**, 3179. (b) Lee, C. H.; La, Y.-H.; Park, J. W. *Organometallics* **2000**, *19*, 344. (c) Nomura, K.; Naga, N.; Takaoki, K. *Macromolecules* **1998**, *31*, 8009. (d) Galka, C. H.; Trösch, D. J. M.; Rüdenauer, I.; Gade, L. H.; Scowen, I. J.; McPartlin, M. *Inorg. Chem.* **2000**, *39*, 4615. (e) Hellmann, K. W.; Galka, C. H.; Rüdenauer, I.; Gade, L. H.; Scowen, I. J.; McPartlin, M. *Angew. Chem., Int. Ed.* **1998**, *37*, 1948.

(4) An example of a W(VI) β-diketiminate complex can be found in: Tonzetich, Z. J.; Jiang, A. J.; Schrock, R. R.; Müller, P. *Organometallics* **2006**, *25*, 4725.

(5) Aoyagi, K.; Gantzel, P. K.; Kalai, K.; Tilley, T. D. *Organometallics* **1996**, *15*, 923.

(6) (a) Pindado, G. J.; Thornton-Pett, M.; Bochmann, M. *J. Chem. Soc., Dalton Trans.* **1998**, 393. (b) Aoyagi, K.; Gantzel, P. K.; Tilley, T. D. *Polyhedron* **1996**, *15*, 4299.

(7) For selected recent examples, see: (a) Hayton, T. W.; Boncella, J. M.; Scott, B. L.; Abboud, K. A.; Mills, R. C. *Inorg. Chem.* **2005**, *44*, 9506. (b) Cameron, T. M.; Gamble, A. S.; Abboud, K. A.; Boncella, J. M. *Chem. Commun.* **2002**, 1148. (c) Mills, R. C.; Abboud, K. A.; Boncella, J. M. *Chem. Commun.* **2001**, 1506. (d) Mills, R. C.; Wang, S. Y. S.; Abboud, K. A.; Boncella, J. M. *Inorg. Chem.* **2001**, *40*, 5077. (e) Cameron, T. M.; Abboud, K. A.; Boncella, J. M. *Chem. Commun.* **2001**, 1224. (f) Cameron, T. M.; Ortiz, C. G.; Ghiviriga, I.; Abboud, K. A.; Boncella, J. M. *Organometallics* **2001**, *20*, 2032. (g) Cameron, T. M.; Ghiviriga, I.; Abboud, K. A.; Boncella, J. M. *Organometallics* **2001**, *20*, 4378. (h) VanderLende, D. D.; Abboud, K. A.; Boncella, J. M. *Organometallics* **1994**, *13*, 3378.

10.1021/om700763v CCC: $37.00 © 2007 American Chemical Society
Publication on Web 11/23/2007

The reactivity of these W species with isocyanate and trimethylaluminum is reported.

Results and Discussion

N,N′-Disubstituted 1,8-diamidonaphthalene (R_2DAN^{2-}) with R as either ^{i}Pr or 3,5-dimethylphenyl was readily introduced to the bis(imido)tungsten framework by reaction between the *in situ* generated dilithium salt, $Li_2[(RN)_2C_{10}H_6]$, and $W(=N^tBu)_2Cl_2(py)_2$ as represented by eq 1.[2a,8] The products of these reactions, $W(=N^tBu)_2[1,8\text{-}(RN)_2C_{10}H_6]py_x$ (**1** R = ^{i}Pr, x = 0; **2** R = 3,5-$Me_2C_6H_3$, x = 1), were obtained in good yields as purple and orange solids, respectively. Hydrocarbon soluble **1** exhibited a ^{1}H NMR spectrum with a broad signal (δ 0.9–1.8) corresponding to the 30 protons for the methyl groups of the combined ^{t}Bu and ^{i}Pr groups and a single septet at 3.95 ppm for the two protons of the ^{i}Pr moieties. The appearance of a single resonance for the methine groups suggested a symmetrical structure based on a tetrahedral ligand array. Compound **2**, while slightly less soluble, also provided ^{1}H and ^{13}C NMR spectra suggesting a symmetrical structure. In particular, the spectra displayed only two distinct signals attributable to the CH_3 groups of the 3,5-dimethylphenyl and the ^{t}Bu groups, respectively. Furthermore, **2** provided NMR and microanalysis data confirming the presence of a single coordinated pyridine group that originated from the starting material. The formula for **2** is reminiscent of the W(IV) DAB complex $W(NPh)(CHCMe_3)(PMe_3)[(Me_3SiN)_2C_6H_4]$.[7d]

The structure of **1** was confirmed through single crystal X-ray

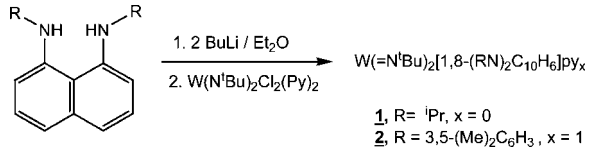

(1)

crystallography with the results displayed in Figure 1.[9,10] The distorted tetrahedral tungsten center possesses an approximate mirror plane of symmetry that bisects the ^{i}Pr$_2$DAN ligand and contains the C(8)−C(13) vector and the W(1), N(3), and N(4) centers. The two $W-N_{amido}$ bond lengths with an average bond length of 1.966 Å are similar to related complexes.[7,11] The short $W-N_{imido}$ bond lengths of 1.771(4) and 1.748(4) Å are consistent with high metal–ligand bond orders (see the Computational Details). A difference between the two imido ligands is reflected in the observed bend angles of 150.6(4) and 169.4(4)°.

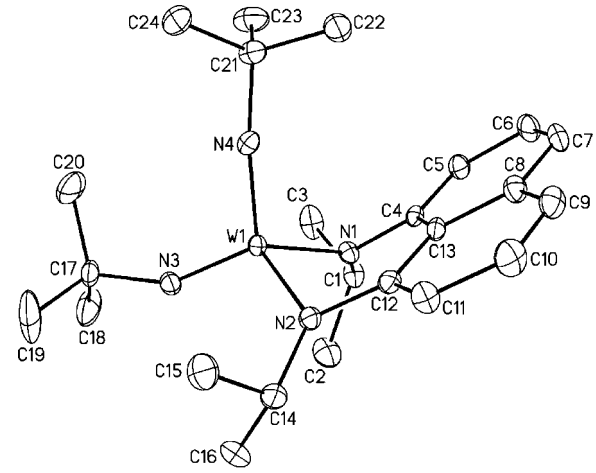

Figure 1. Thermal ellipsoid plot showing the molecular structure and atom numbering scheme for one of the independent molecules of **1**.[9] Hydrogen atoms have been omitted for clarity.

Perhaps the most notable structural feature for **1** is the nonplanar coordination of the ^{i}Pr$_2$DAN^{2-} ligand. The fold angle of 122.6° between the naphthyl moiety and the N(1)−W(1)−N(2) planes positions the W atom ca. 1.14 Å out of the naphthyl plane. This feature causes the methyl groups on the ^{i}Pr substituents to be crystallographically distinct. The appearance of a single ^{i}Pr group in the NMR spectra of **1** suggests fluxionality on this time scale. Interestingly, the N(1) and N(2) centers are planar (Σ angles = 359°). This structural feature of **1** closely parallel the reported Sn(II) compound of this ligand[2a] and is similar to the distortions observed in R_3SiDAB^{2-} complexes. However, the mononuclear structure of **1** is in contrast with the imido-bridged dimer observed for the closely the related bis(imido)Mo(Me_3SiDAB) species $[Mo(NPh)(\mu\text{-}NPh)(o\text{-}(Me_3SiN)_2C_6H_4)]_2$.[12] Furthermore, the structure of [*N*,*N*′-bis(trimethylsilyl)-6,6′-dimethylbipheny]-2,2′-diamido]bis(2,6-diisopropylphenylimido)tungsten(VI) displays a symmetrical albeit twisted biphenyldiamido ligand.[13]

The apparent ligand distortion observed for complex **1** was probed through Gaussian 03[14] DFT calculations using the B3LYP functional[15] and the SDD and LANL2DZ basis sets.[16] An optimization that began from a symmetrical C_{2v} structure for **1** possessing a planar ^{i}Pr$_2$DAN^{2-} ligand led to a C_s-symmetric structure that represents a true energy minimum (all positive harmonic frequencies) and is closely correlated with the experimentally obtained structure as shown in Figure 2. Furthermore, the low-symmetry structure was calculated to be approximately 15 kcal mol^{-1} more stable than the C_{2v} structure.[17] These results indicate that the observed structure for **1** is indeed the preferred minimum even in the absence of crystal packing forces. An analysis of the fragment orbital interactions[18] for the R_2DAN^{2-} and $W(NR)_2^{2+}$ fragments in the complex

(8) Bazinet, P.; Ong, T.-G.; O'Brien, J. S.; Lavoie, N.; Bell, E.; Yap, G. P. A.; Korobkov, I.; Richeson, D. S. *Organometallics* **2007**, *26*, 2885.

(9) For simplicity, discussion has been limited to only one of the two independent units of **1** in the unit cell. There are no significant differences in the bond lengths and angles between these two species.

(10) Complex **1**: T = 120 K, l = 0.71073 Å, triclinic, space group P-1, a = 9.860(4) Å, b = 14.171(5) Å, c = 18.738(7) Å, α = 98.619(6)°, β = 102.019(6)°, γ = 93.095(6)°, V = 2522.0(16)Å^3, Z = 4, final R indices [$I > 2\sigma(I)$] R1 = 0.0363, wR2 = 0.0893. Complex **3b**: T = 213 K, l = 0.71073 Å, monoclinic, space group $P2_1/c$, a = 18.090(3) Å, b = 10.2206(14) Å, c = 22.508(3) Å, β = 110.758(2)°, V = 3891.4(9) Å^3, Z = 4, final R indices [$I > 2\sigma(I)$] R1 = 0. 0428, wR2 = 0. 0885. Complex **4a**: T = 200 K, l = 0.71073Å, triclinic, space group P-1, a = 10.6792(18) Å, b = 11.713(2) Å, c = 15.218(3) Å, α = 84.744(3)°, β = 78.196(3)°, γ = 75.125(3)°, V = 1799.2(5) Å^3, Z = 2, final R indices [$I > 2\sigma(I)$] R1 = 0.0270, wR2 = 0.0736.

(11) (a) Ward, B. D.; Orde, G.; Clot, E.; Cowley, A. R.; Gade, L. H.; Mountford, P. *Organometallics* **2005**, *24*, 2368. (b) Ward, B. D.; Orde, G.; Clot, E.; Cowley, A. R.; Gade, L. H.; Mountford, P. *Organometallics* **2004**, *23*, 4444.

(12) Ortiz, C. G.; Abboud, K. A.; Boncella, J. M. *Organometallics* **1999**, *18*, 4253.

(13) Mills, R. C.; James, M.; Boncella, J. M.; Abboud, K. A. *Acta Crystallogr.* **2001**, *E57*, m218.

(14) Frisch, M. J.,et al. Gaussian 03, Revision D.01, Gaussian, Inc.: Wallingford, CT, 2004.

(15) (a) Becke, A. D. *J. Chem. Phys.* **1993**, *98*, 5648. (b) Lee, C.; Yang, W.; Parr, R. G. *Phys. Rev. B* **1988**, *37*, 785.

(16) Hay, P. J.; Wadt, W. R. *J. Chem. Phys.* **1985**, *82*, 299.

(17) These results are summarized in Figures S3–S5 that are provided in the Supporting Information.

(18) (a) Gorelsky, S. I.; Ghosh, S.; Solomon, E. I. *J. Am. Chem. Soc.* **2006**, *128*, 278. (b) Gorelsky, S. I. AOMix software for molecular orbital analysis, www.sg-chem.net.

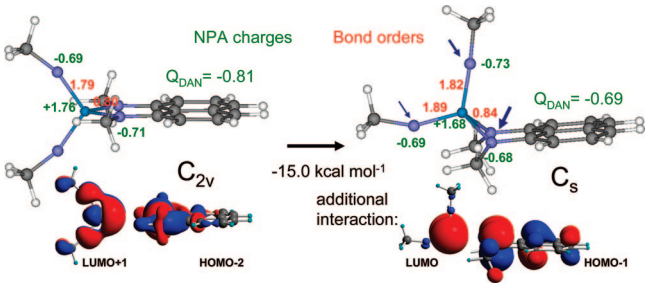

Figure 2. Calculation results for compound **1** with both C_{2v} and C_s symmetry. Mayer bond orders and NPA[20] atomic charges for the two structures at the B3LYP/SDD level of theory are depicted in red and green labels, respectively. Dark blue arrows indicate the sites of potential isocyanate reaction as described in the text. The size of the arrow indicates the relative thermodynamic preference of reaction determined from the computations. The most important orbital interactions between fragments are depicted.

indicates that the four highest occupied fragment orbitals (HOMO to HOMO-3) of the diamidonaphthalene ligand and the five lowest unoccupied fragment orbitals (LUMO to LUMO+4) of the $W(NR)_2^{2+}$ fragment are involved in covalent bonding for complex **1** (Figure S4, Supporting Information). For the complex with C_{2v} symmetry, the donor HOMO-1 (π orbital) of the R_2DAN^{2-} ligand can interact with LUMO+4 of $W(NR)_2^{2+}$. The observed bend of the diamidonaphthalene ligand allows overlap between this donor orbital with low-energy, W 5d-based acceptor orbitals (LUMO and LUMO+2, Figure S5, Supporting Information), thus increasing the metal–ligand interaction through increased π donation from the amido N atoms to these two σ-type acceptor orbitals of the metal fragment (their electron populations increase from 18.0% for the LUMO and 6.5% for LUMO+2 in the C_{2v} structure to 25.3% and 14.8% in the C_s structure, respectively). This, in turn, reduces the W atomic charge, increases the bond order for the $W-N_{imido}$ linkages, and leads to the crystallographically observed differences in the two imido moieties. Related observations regarding the increased charge donation have been reported from computational investigations on diamidobenzene complexes.[19] However, these studies did not report that the ligand distortion generates significantly improved overlap between the donor occupied orbital of the ligand and the lowest energy acceptor orbitals of the metal fragment which leads to the observed gain in energy.

The computed electron distribution for **1** may presage the reactivity of this species. In particular, the increased electron density on the imido groups concomitant with the reduced charges on the $^iPr_2DAN^{2-}$ moiety and the W center (Figure 2) in the low-symmetry structure suggested the potential for increased reactivity of the imido ligands and prompted our exploration of addition reactions of **1** and **2** involving *p*-tolyl isocyanate and alkylation reactions of these compounds using Al_2Me_6. We began by examining the relative site selectivity, toward isocyanate, for the amido and imido functions of **1** computationally and experimentally. Possible ureato products of this reaction, $[(RN)C_{10}H_6(R'N)C(=O)NR]W(N^tBu)_2$ and $[C_{10}H_6(NR)_2]W(^tBuNC(=O)NR')(N^tBu)$, could arise from insertion into the $W-N_{amido}$ or addition to the $W=N_{imido}$ groups respectively (Figure 2, dark blue arrows). Optimizations of these products at the B3LYP/SDD level generated structures that were confirmed to be minima and with a preference for the amido insertion product of between 6.4 and 15.8 kcal mol^{-1} depending on the isomer used in the computation.[21]

Treatment of either **1** or **2** with *p*-tolyl isocyanate proceeded to yield the predicted ureato compounds $[(RN)C_{10}H_6(Ar'N)C(=O)NR]W(N^tBu)_2$ ($Ar' = p\text{-}MeC_6H_4$; R= ^{i}Pr **3a**, 3,5-$Me_2C_6H_3$ **3b**) (Scheme 1). The unsymmetrical nature of these species was demonstrated by the ^1H and ^{13}C spectra, which in both cases displayed two unique N^tBu and two NR resonances. Definitive structural details of **3a** and **3b** were provided by single-crystal X-ray diffraction studies. The results of these analyses unambiguously established the similarity of these products and the fact that they arose from the insertion of the isocyanate into amido W−N bond of the starting materials.[22] These observations are consistent with the computational results and with the fact that amido-supported group 6 imido complexes generally undergo preferential reaction of isocyanate with the amido function.[7,11,23,24]

Examining the structure of **3b** confirms the transformation one of the original amido groups of the R_2DAN^{2-} ligand into an *N,N'*-ureato ligand.[10] The coordination geometry for this compound can be described as distorted square-based pyramidal with one of the N^tBu imido groups (N5) occupying the axial position. The imido W−N bond lengths are slight shorter (W(1)−N(4) 1.753(5) Å, W(1)−N(5) 1.739(5) Å) and more linear (average angle 167.4(4)°) than in **1**. The remaining W−N bonds span the anticipated range with W(1)−N(3) being the shortest amido linkage of 2.034(4) Å followed by W(1)−N(1) 2.129(5) Å and then the dative interaction W(1)−N(2) 2.300(5) Å.[23,25]

Compounds **1** and **2** both react with trimethylaluminum to alkylate the W center and to incorporate the resulting Me_2Al moiety into the complex via the diamidonaphthalene group. For example, treatment of a diethyl ether solution of **1** with ~5 equiv of Al_2Me_6 resulted in a pale yellow solution after 8 h. Colorless crystals of these products were isolated from hexane and were subjected to X-ray diffraction analysis.[22]

The bimetallic structure obtained for **4a** is depicted in Scheme 1 and consists of a distorted square pyramidal W complex and a pseudotetrahedral Al center which are bridged by the R_2DAN^{2-} amido linkage.[10] The imido center N(3) resides in the apical position and, while this group is less linear than the other imido group (C(20)−N(3)−W(1) 154.9(5)°, C(24)−N(4)−W(1) 175.7(4)°), both $W=N_{imido}$ bond distances remain short (W(1)−N(3) 1.755(5) Å, W(1)−N(4) 1.744(5) Å) and correspond to triple bonds, thus providing an 18-electron configuration to W. The amido N centers are quaternary in compound **4** and, therefore, display longer W−N distances (W(1)−N(1) 2.237(5) Å, W(1)−N(2) 2.361(5) Å) than in the starting material.

(19) (a) Galindo, A.; del Rýo, D.; Mealli, C.; Ienco, A.; Bo, C. *J. Organomet. Chem.* **2004**, *689*, 2847. (b) Galindo, A.; Ienco, A.; Mealli, C. *Comments Inorg. Chem.* **2002**, *23*, 401. (c) Galindo, A.; Ienco, A.; Mealli, C. *New J. Chem.* **2000**, *24*, 73.

(20) Reed, A. E.; Weinstock, R. B.; Weinhold, F. *J. Chem. Phys.* **1985**, *83*, 735.

(21) Computational details for the ureato products can be found in the Supporting Information.

(22) The structures of **3a** and **3b** are analogous and discussion will be limited to that of **3b**. A thermal ellipsoid plot for **3a** as well as the CIF file for this structure can be found in the Supporting Information. The structures of **4a** and **4b** are analogous and discussion will be limited to that of **4a**. A thermal ellipsoid plot for **4b** as well as the cif file for this structure can be found in the Supporting Information.

(23) Lam, H. W.; Wilkinson, G.; Hussain-Bates, B.; Hursthouse, M. B. *J. Chem. Soc., Dalton Trans.* **1993**, 781.

(24) For an example of cycloaddition of isocyanates with tungsten imides, see: Legzdins, P.; Phillips, E. C.; Rettig, S. J.; Trotter, J.; Veltheer, J. E.; Yee, V. C. *Organometallics* **1992**, *11*, 3104.

(25) Rische, D.; Baunemann, A.; Winter, M.; Fischer, R. A. *Inorg. Chem.* **2006**, *45*, 269.

Scheme 1

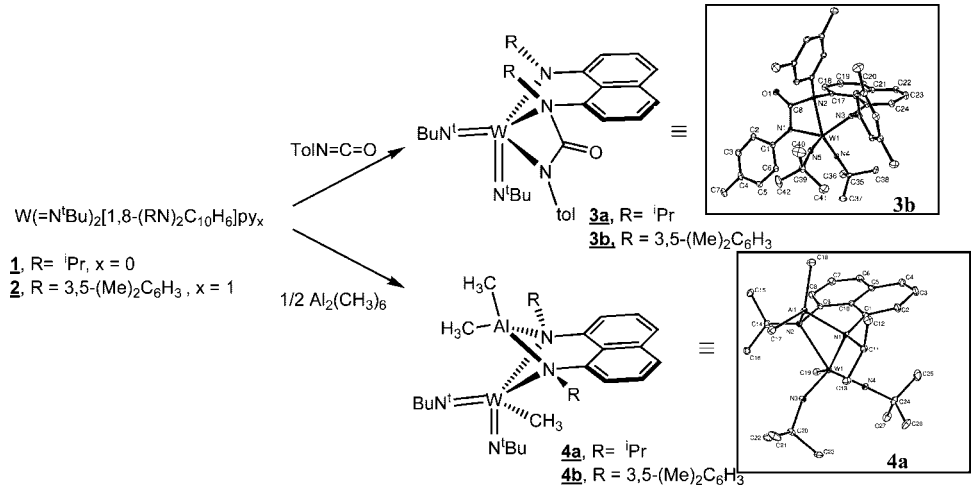

The longer W−N(2) bond distance is oriented trans to the imido-N(4) group. The coordination sphere of W is completed by a methyl group that originated from the Al starting material (W(1)−C(19) 2.172(6) Å). The approximately tetrahedral Al environment with average angles of 108.9(3)° consists of two methyl groups and the two bridging amido functions.

The diamido-bridged heterobimetallic species **4a** and **4b** contrast with recent reports of transmetalation reactions between trimethylaluminum and related Zr(IV) and Mo(VI) amido species. For example, the *o*-diamidobenzene species, (Mo(NPh)(*o*-(SiMe$_3$N)$_2$C$_6$H$_4$)(CH$_2$)$_4$ and (Mo(NPh)(*o*-(SiMe$_3$N)$_2$C$_6$H$_4$)(PhCCPh), reacted with Al$_2$Me$_6$ to undergo complete transfer of the diamido ligand to the Al and formation of a π-complex of the resultant [Me$_2$Al(*o*-(SiMe$_3$N)$_2$C$_6$H$_4$)]$^-$ with the Mo center.[26] Complexes of the type (R-IAN)$_2$ZrNMe$_2$, where IAN is a bidentate N,N′ ligand formally of the β-diketiminate class, readily transmetalate to aluminum to give (R-IAN)AlMe$_2$ and Me$_2$Zr(NMe$_2$)$_2$ as products.[27] In the case of products **4a** and **4b**, the transfer reaction is apparently arrested at the formation of the diamido bridged Al/W complex. The lengthened W−N$_{amido}$ linkages of **4a/b** in combination with the short Al−N bond lengths does support a zwitterionic contribution, with cationic W and anionic Al components, to the bonding in these compounds.

This first application of the N,N′-disubstituted 1,8-diamidonaphthalene framework (R$_2$DAN^{2-}) with a high-valent W(VI) metal center has been examined through structural, computational, and reactivity studies. Computationally, the observed bonding features of this ligand array revealed the structural features that manifest themselves to allow for a flexible and increased ligand-to-metal π-electron donation. Computational and experimental analysis of the reactivity of these species with isocyanate demonstrated insertion into one of the W−N$_{amido}$ bonds and formation of the *N*,*N*′-ureato species. Alkylation of the W centers of **1** and **2** with Al$_2$Me$_6$ and the incorporation of the Lewis acid AlMe$_2^+$ products through the diamidonaphthalene groups are consistent with the electron distribution of the starting materials and reveal the ability of the R$_2$DAN^{2-} ligand to construct heterobimetallic species. Our continuing studies seek to reveal the broader aspects of the R$_2$DAN^{2-} framework as a reaction site and the ability to provide support for reactive metal complexes.

(26) Ison, E. A.; Abboud, K. A.; Ghiviriga, I.; Boncella, J. M *Organometallics* **2004**, *23*, 929.

(27) Cortright, S. B.; Coalter, J. N., III; Pink, M.; Johnston, J. F. *Organometallics* **2004**, *23*, 5885.

Experimental Section

General Methods. Reactions were performed using standard Schlenk techniques (N$_2$) or, alternatively, in a glovebox with a nitrogen atmosphere. Unless otherwise noted, solvents were sparged with nitrogen and then dried by passage through a column of activated alumina using an apparatus purchased from Anhydrous Engineering. Deuterated benzene was dried using activated molecular sieves. WCl$_6$ and 1,8-diaminonaphthalene were purchased from Aldrich and used without further purification. *N*,*N*′-Diisopropyl 1,8-diaminonaphthalene and *N*,*N*′-bis(3,5-dimethylphenyl)-1,8-diaminonaphthalene were prepared according to a previously reported procedures.[2,8] WCl$_2$(N^{t}Bu)$_2$Cl$_2$(Py)$_2$ was prepared according to the literature.[25] NMR spectra were run on either a Gemini 200 MHz or a Bruker 300 or 500 MHz spectrometer with deuterated benzene as a solvent and internal standard. All elemental analyses were carried out by Guelph Chemical Laboratories, Ltd. in Ontario, Canada.

Preparation of W(N^{t}Bu)$_2$[1,8-(^{i}PrN)$_2$C$_{10}$H$_6$] (1). Addition of 1.6 M BuLi (5.3 mL, 8.46 mmol) to a solution of 1,8-(^{i}PrNH)$_2$C$_{10}$H$_6$ (1.03 g, 4.23 mmol) in 30 mL of diethyl ether led to an immediate color change of the solution to green and then to brown with gas evolution. To this reaction mixture was added W(N^{t}Bu)$_2$Cl$_2$(py)$_2$ (2.35 g, 4.23 mmol), which was allowed to stir for 8 h. The solvent was then evaporated under vacuum, and the solid was extracted with hexane to yield **1** as a purple solid (1.70 g, 74%). ^{1}H NMR (C$_6$D$_6$, 200 MHz,): δ 0.9–1.8 (br overlapping signals, 30 H, CH$_3$ from ^{t}Bu and ^{i}Pr groups), 3.97 (sept, 2H, CHMe$_2$), 6.53 (d, 2H, Ar-H), 7.15 (m, 4H, Ar-H). ^{13}C NMR (C$_6$D$_6$, 500 MHz): δ 25.4 (*C*H$_3$), 27.6 (*C*H$_3$), 33.8 (*C*H), 55.4(*C*Me$_3$), 111.9 (CH), 122.4 (C), 127.8 (CH), 130.1 (CH), 138.5 (C), 151.4 (C). Anal. Calcd for C$_{24}$H$_{38}$N$_4$W: C, 50.89; H, 6.76; N, 9.89. Found: C, 50.59; H, 6.91; N, 9.59.

Preparation of W(N^{t}Bu)$_2$[1,8-(2,6-Me$_2$C$_6$H$_3$NH)$_2$C$_{10}$H$_6$] py (2). Using a procedure similar to the synthesis of **1** with 1.6 M BuLi (1.35 mL, 2.17 mmol), 1,8-(2,6-Me$_2$C$_6$H$_3$NH)$_2$C$_{10}$H$_6$ (398 mg, 1.09 mmol), and W(N^{t}Bu)$_2$Cl$_2$(py)$_2$ (603 mg, 1.09 mmol) produced compound **2** as an orange powder (716 mg, 85.7%). ^{1}H NMR (C$_6$D$_6$, 200 MHz): δ 1.07 (s, 18H, CCH$_3$), 2.11 (s, 12H, C$_{Ar}$CH$_3$), 6.45–6.89 (m, 7H, Ar-H), 6.97 (s, 4H, Ar-H), 7.26–7.31 (m, 4H, Ar-H), 8.90 (d, 2H, py). ^{13}C (C$_6$D$_6$, 200 MHz): δ 21.49 (*C*H$_3$), 32.36 (*C*H$_3$), 67.91 (*C*Me$_3$), 116.18 (C), 121.13 (CH), 121.92 (CH), 123.43 (CH), 124.17 (CH), 126.31 (CH), 128.31 (CH), 137.62 (C), 137.91 (C), 138.35 (CH),150.45 (C),152.00 (CH), 156.48 (C). Anal. Calcd for C$_{39}$H$_{47}$N$_5$W: C, 60.86; H, 6.16; N, 9.10 Found: C, 60.94; H, 5.80; N, 8.69.

Reaction of $W(N^tBu)_2[1,8\text{-}(^iPrN)_2C_{10}H_6]$ with $MeC_6H_4N{=}C{=}O$ (3a). To a solution of **1** $W(NtBu)_2[1,8\text{-}(^iPrN)_2C_{10}H_6]$ (0.320 g, 0.594 mmol) in 30 mL of ether was added $MeC_6H_4N{=}C{=}O$ (0.095 g, 0.713 mmol). After the reaction mixture was stirred overnight, the volatiles were removed under vacuum and the resultant solid was redissolved in 10 mL of hexane. Insoluble solid was removed by filtration and the filtrate was cooled to −30 °C to afford microcrystals of **3a** (0.211 g, 52.9%). ^{1}H NMR (C_6D_6, 500 MHz): δ 0.77 (s, 9H, CH_3), 1.20 (d, 3H, CH_3), 1.26 (s, 9H, CH_3), 1.45 (d, 3H, CH_3), 1.63 (d, 3H, CH_3), 1.71 (d, 3H, CH_3), 2.08 (s, 3H, CH_3), 3.90 (qq, 1H, CH), 4.63 (qq, 1H, CH), 6.98 (d, 1H, Ar-H), 7.02 (t, 1H, Ar-H), 7.03 (d, 2H, Ar-H), 7.18 (d, 1H, Ar-H), 7.36 (t, 1H, Ar-H), 7.49 (d, 1H, Ar-H), 8.02 (d, 2H, Ar-H), 8.17 (d, 1H, Ar-H). ^{13}C NMR (C_6D_6, 500 MHz): 18.3 (*C*H_3), 20.9, 21.6, 23.6, 26.0 (*C*H_3), 32.2, 33.1 (*C*H_3), 56.5, 58.0 (*C*H), 67.9(*C*Me_3), 67.6 (*C*Me_3), 111.2 (C), 119.3 (CH), 119.8 (CH), 122.4 (C), 124.8 (CH), 124.9 (CH), 127.1 (CH), 128.9 (CH), 129.5 (CH), 133.8 (CH), 136.8 (C), 137.7 (C), 143.0 (C), 152.4 (C), 156.9 (*C*O). Anal. Calcd for $C_{32}H_{45}N_5OW$: C, 54.94; H, 6.48; N, 10.01. Found: C, 55.11; H, 6.61; N, 9.87.

Reaction of $W(N^tBu)_2[1,8\text{-}(2,6\text{-}Me_2C_6H_3NH)_2C_{10}H_6]$py with TolN=C=O (3b). Following a procedure similar to the synthesis of **3a** using **2** $W(N^tBu)_2[1,8\text{-}(2,6\text{-}Me_2C_6H_3NH)_2C_{10}H_6]$py (0.200 g, 0.26 mmol) and *p*-tolyl isocyanate (0.035 g, 0.26mmol) produced compound **3b** as a beige powder (0.117 g, 54.6%). ^{1}H NMR (C_6D_6, 200 MHz): δ 1.01 (s, 9H, CH_3), 1.10 (s, 9H, CH_3), 1.82 (s, 6H, CH_3), 2.09 (s, 3H, CH_3), 2.14 (s, 6H, CH_3), 6.24 (s, 2H, Ar-H), 6.65 (m, 3H, Ar-H) 7.15 (m, 7H, Ar-H), 7.57 (d, 1H, Ar-H), 8.25 (d, 2H, Ar-H), 8.56 (d, 1H, Ar-H). ^{13}C (C_6D_6, 200 MHz): δ 20.9 (CH_3), 21.0 (*C*H_3), 21.2 (*C*H_3), 31.9 (*C*H_3), 32.8 (*C*H_3), 67.6 (*C*Me_3), 67.7 (*C*Me_3), 115.0 (CH), 119.4 (CH), 119.9 (C), 121.9 (C), 122.7 (CH), 124.2 (CH), 125.6 (CH), 125.8 (CH), 126.9 (CH), 128.3 (CH), 128.7 (C), 129.0 (CH), 130.0 (CH), 134.0 (C), 135.7 (C), 136.6 (C), 138.2 (CH), 139.0 (CH), 142.9 (C), 145.5 (C), 151.9 (C), 156.6 (C), 157.8 (CO). Anal. Calcd for $C_{42}H_{49}N_5OW$: C, 61.24; H, 6.00; N, 8.50. Found: C, 60.92; H, 6.23; N, 8.08.

Reaction of $W(N^tBu)_2[1,8\text{-}(^iPrN)_2C_{10}H_6]$ with Al_2Me_6 (4a). In a round-bottom flask equipped with a magnetic stir bar **1a** (0.411 g, 0.764 mmol) was dissolved in hexanes, trimethylaluminum (0.165 g, 2.28 mmol) was added to this solution. The reaction mixture was stirred for 6 h and then dried under vacuum. The yellow solid was recrystallized from hexanes to give clear crystals (0.150 g, 31%). ^{1}H NMR (C_6D_6, 300 MHz, 50 °C): δ −1.20 (s, 3H, CH_3), 0.23 (s, 3H, CH_3), 0.41 (br s, 3H, CH_3), 0.91 (br s, 9H, *t*Bu), 1.28 (br, 3H, CH_3), 1.41 (s, 9H, *t*Bu), 1.78 (br, 6H, CH_3), 2.02 (d, 3H, CH_3), 3.86 (br m, 2H, CH) 6.86 (d, 1H), 6.96 (d, 1H), 7.32 (m, 4H). ^{13}C (C_6D_6, 300 MHz): δ −7.0 (br, CH_3,AlMe), −0.05 (br, CH_3, AlMe), 18.7 (CH_3, WMe) 21.4 (CH_3), 22.5 (CH_3), 25.7 (CH_3), 27.2 (CH_3), 31.5 (CH_3, *t*Bu), 32.2 (CH_3, *t*Bu), 66.7 (C, *t*Bu), 66.9 (C, *t*Bu), 112.1 (CH), 120.3 (C), 122.9 (CH), 124.3 (CH), 126.3 (C), 127.3 (CH), 127.4 (CH), 137.1 (CH), 147.0 (C), 148.0 (C). Anal. Calcd for $C_{27}H_{47}AlN_4W$: C, 50.79; H, 7.42; N, 8.77. Found: C, 50.54; H, 7.65; N, 8.67.

Reaction of $W(N^tBu)_2[1,8\text{-}(2,6\text{-}Me_2C_6H_3NH)_2C_{10}H_6]$py with $Al(Me)_3$ (4b). Using a procedure similar to the synthesis of **4a** using **1b** (0.330 g, 0.43 mmol) and trimethylaluminum (0.074 g, 1.03 mmol) produced compound **4b** as light purple crystals (0.095 g, 28%). ^{1}H NMR (C_6D_6, 300 MHz): δ −0.55 (s, 3H, CH_3), −0.39 (s, 3H, CH_3), 0.73 (s, 3H, CH_3), 0.92 (s, 9H, *t*Bu), 1.50 (s, 9H, *t*Bu), 2.07 (s, 6H, CH_3), 2.33 (s, 6H, CH_3), 7.37–6.60 (m, 10H), 8.00 (s, 1H),8.37–8.29 (m br, 1H). ^{13}C (C_6D_6, 300 MHz) δ −9.17 (CH_3,AlMe), −7.96 (CH_3, AlMe), 21.6 (CH_3), 22.0 (CH_3, WMe), 22.8 (CH_3), 31.4 (CH_3, *t*Bu), 32.7 (CH_3, *t*Bu), 66.9 (C, *t*Bu), 67.8 (C, *t*Bu), 114.3 (CH), 115.3 (CH), 119.4 (C), 123.3 (CH), 124.2 (CH), 125.2 (C), 125.4 (C), 127.3 (CH), 127.4 (CH), 127.5 (CH), 129.0 (C), 137.1 (C), 139.4 (C), 139.6 (C), 145.2 (CH), 146.6 (CH),147.6 (CH), 149.0 (C). Anal. Calcd for $C_{37}H_{51}AlN_4W$: C, 58.27; H, 6.74; N, 7.35. Found: C, 57.85; H, 6.92; N, 7.15.

Computational Details. DFT calculations with the B3LYP functional were carried out using the Gaussian 03 (revision D.01) suite of programs. Spin-restricted treatment was used for all closed-shell species. The basis sets SDD and LANL2DZ were employed. In the case of complex **1**, a symmetrical C_{2v} structure was prepared and used as the staring point in optimizations with both SDD and LANL2DZ basis sets. Both cases resulted in the same minimum structure of lower (C_s) symmetry that was similar to the experimentally obtained crystal structure. Frequency calculations on the optimized structures were used to compare the thermodynamic stability of the C_{2v} and C_s structures. Atomic charges were calculated by natural population analysis (NPA) as implemented in Gaussian 03. Mayer bond orders were obtained using the AOMix-L program. The analysis of molecular orbitals (MOs) in terms of fragment orbital (FO) contributions and calculations of the FO overlap matrices and FO populations were carried out using the AOMix-CDA program. The converged wave functions were tested to confirm that they represent to the true ground state.

Three possible ureato products of the reaction of complex **1** and *p*-tolyl isocyanate were prepared with GaussView and were used as the starting points in the optimization calculations for these species using the SDD basis set. In all cases, the default optimization conditions were employed. Frequency calculations on these optimized structures were used to confirm that the computed structures were indeed minima and in the calculation of the relative thermodynamic stabilities of these species.

Acknowledgment. This work was supported by NSERC.

Supporting Information Available: An extended summary of the computational methods employed and a complete citation to ref 14. Thermal ellipsoid plots for **3a** and **4b**. Results for the optimization of **1**, the fragment orbital interactions for this species, and the atomic coordinates of optimized structures. A crystallographic file (CIF) for compounds **1**, **3a**, **3b**, **4a**, **4b**. This material is available free of charge via the Internet at http://pubs.acs.org.

OM700763V